© 2018. Published by The Company of Biologists Ltd | Journal of Cell Science (2018) 131, jcs213876. doi:10.1242/jcs.213876

RESEARCH ARTICLE

# Lipid droplet consumption is functionally coupled to vacuole homeostasis independent of lipophagy

**Sarah Ouahoud[1,2,*], Mitchell D. Fiet[1,2,*], Fernando Martínez-Montañés[3], Christer S. Ejsing[3,4], Oliver Kuss[2,5], Michael Roden[1,2,6] and Daniel F. Markgraf[1,2,‡]**

## ABSTRACT

Lipid droplets (LDs) store neutral lipids and are integrated into a cellular metabolic network that relies on functional coupling with various organelles. Factors mediating efficient coupling and mechanisms regulating them remain unknown. Here, we conducted a global screen in *S. cerevisiae* to identify genes required for the functional coupling of LDs and other organelles during LD consumption. We show that LD utilization during growth resumption is coupled to vacuole homeostasis. ESCRT-, V-ATPase- and vacuole protein sorting-mutants negatively affect LD consumption, independent of lipophagy. Loss of ESCRT function leads to the accumulation of LD-derived diacylglycerol (DAG), preventing its conversion into phosphatidic acid (PA) and membrane lipids. In addition, channeling of DAG from LD-proximal sites to the vacuole is blocked. We demonstrate that utilization of LDs requires intact vacuolar signaling via TORC1 and its downstream effector Sit4p. These data suggest that vacuolar status is coupled to LD catabolism via TORC1-mediated regulation of DAG-PA interconversion and explain how cells coordinate organelle dynamics throughout cell growth.

**KEY WORDS: Lipid metabolism, Lipid droplet, Diacylglycerol, Vacuole homeostasis, ESCRT, TORC1**

## INTRODUCTION

Cells store energy as fat in specific organelles, the lipid droplets (LDs). They consist of a core of neutral lipids, such as triacylglycerols (TAGs) and sterol esters (SE), which is surrounded by a phospholipid monolayer (Fujimoto and Parton, 2011; Leber et al., 1994; Penno et al., 2013). As key players in lipid metabolism LDs are implicated in the most frequent human metabolic disorders, i.e. obesity, type 2 diabetes and non-alcoholic fatty liver disease (Gluchowski et al., 2017; Markgraf et al., 2016; Tilg et al., 2017). LDs were shown to dynamically interact with a variety of cellular organelles, i.e. the endoplasmic reticulum (ER), mitochondria, vacuoles (mammalian lysosomes) and peroxisomes (Barbosa and Siniossoglou, 2017; Kohlwein et al., 2013; Walther and Farese, 2012). How this dynamic metabolic network is regulated and coordinated is only poorly understood.

Budding yeast *Saccharomyces cerevisiae* is a valuable model organism to study LD dynamics. LDs grow in size and number due to increased TAG synthesis when cells enter stationary phase. Utilization of LDs is driven by the hydrolysis of TAGs during growth resumption (Kurat et al., 2006). The formation of LDs is initiated in the ER, where activated fatty acids (FA-CoA) are converted to TAG in sequential reactions, catalyzed by members of highly conserved enzyme families (Buhman et al., 2001; Czabany et al., 2007; Natter et al., 2005). The key intermediate diacylglycerol (DAG) is generated in the ER from phosphatidic acid (PA) by the PA hydrolase Pah1p and can be converted to TAG by two diacylglycerol-acyl transferases, Lro1p and Dga1p (Adeyo et al., 2011; Oelkers et al., 2002). During growth resumption, lipases such as Tgl3p hydrolyze TAGs to initiate LD consumption (Kurat et al., 2006). The subsequent channeling of lipolysis products, i.e. FAs and DAG into compartmentalized downstream pathways depends on the functional coupling of LDs and other organelles. DAG is channeled from LDs into the ER for re-esterification to TAG and subsequent assembly of lipoprotein particles in the liver (Lankester et al., 1998; Wiggins and Gibbons, 1992). DAG is also an important precursor for membrane lipid biosynthesis in the ER. In the cytidine diphosphate (CDP)-DAG pathway, DAG is converted to PA, by the diacylglycerol kinase Dgk1p and subsequently to phospholipids, such as phosphatidylserine (PS), phosphatidylthanolamine (PE), phosphatidylcholine (PC) and phosphatidylinositol (PI) (Fakas et al., 2011; Han et al., 2008). The channeling of DAG from LDs to the ER for membrane lipid biosynthesis requires the ER protein Ice2p (Markgraf et al., 2014).

LDs were shown to interact with vacuoles in yeast and lysosomes in mammalian cells. In addition to the activity of LD-localized lipases, lipophagy, a special form of autophagy, plays an important role in the mobilization of FAs from LDs during starvation in hepatocytes (Singh et al., 2009). In yeast, LDs can be utilized via microautophagy upon nitrogen starvation or entry into stationary phase. LDs that directly associate with vacuoles are internalized and degraded by resident hydrolases, utilizing the core autophagy machinery (van Zutphen et al., 2014; Wang, 2014; Wang et al., 2014). In contrast, ESCRT-dependent microautophagy is induced after diauxic shift and does not require the core autophagy machinery but the vacuolar lipase Atg15p (Oku et al., 2017).

Interestingly, key intermediates in the formation and consumption of TAGs, i.e. DAG and PA, were shown to affect the dynamics of vacuoles by influencing fusion and fission reactions of this organelle (Mima et al., 2008; Starr et al., 2016). In fact, the enzymes interconverting DAG and PA, Dgk1p and Pah1p, localize to the vacuole (Miner et al., 2017; Sasser et al., 2012). However, how the interplay between these two highly dynamic organelles is coordinated throughout the cell cycle is not understood.

[1]Institute for Clinical Diabetology, German Diabetes Center, c/o Auf'm Hennekamp 65, D-40225 Düsseldorf, Germany. [2]German Center for Diabetes Research (DZD e.V.), München, Neuherberg, Germany. [3]Department of Biochemistry and Molecular Biology, Villum Center for Bioanalytical Sciences, University of Southern Denmark, 5230 Odense, Denmark. [4]Cell Biology and Biophysics Unit, European Molecular Biology Laboratory, D-69117 Heidelberg, Germany. [5]Institute for Biometrics and Epidemiology, German Diabetes Center, Auf'm Hennekamp 65, D-40225 Düsseldorf, Germany. [6]Division of Endocrinology and Diabetology, Medical Faculty, Heinrich-Heine University, D-40225 Düsseldorf, Germany.
*These authors contributed equally to this work

‡Author for correspondence (daniel.markgraf@ddz.uni-duesseldorf.de)

M.D.F., 0000-0001-6669-5368; D.F.M., 0000-0002-2252-8442

**Received 7 December 2017; Accepted 13 April 2018**

Journal of Cell Science (2018) 131, jcs213876. doi:10.1242/jcs.213876

Here, we report the identification of proteins required for integrating LDs into a metabolic network during growth resumption. By implementing a flow-cytometry-based genome-wide screen in yeast, *S. cerevisiae*, we show that LD consumption is coupled to ESCRT function and vacuole homeostasis, independently of autophagy. Abolishing ESCRT function affects the conversion of LD-derived DAG into PA and membrane lipids and its channeling towards vacuoles. Our data suggest that a nonfunctional late-endosomal/vacuolar system halts utilization of LD-derived DAG by TORC1-mediated regulation of enzymes involved in DAG-PA interconversion.

## RESULTS

### A genome-wide screen for regulators of LD dynamics

Genome-wide screens in various organisms analyzed the size, number and morphology of BODIPY493/503-labeled LDs at specific growth states, mainly by using fluorescence microscopy (Fei and Yang, 2012; Guo et al., 2008; Szymanski et al., 2007). However, such analyses are laborious, rely on manual inspection and, as such, are unsuitable for the quantitative screening of a large number of regulators of LD dynamics at multiple time points. Here, we established a flow cytometry-based high throughput method to analyze BODIPY493/503-labeled LDs during growth resumption. LDs of fixed wild-type cells and cells lacking the main lipase Tgl3p (*tgl3*Δ cells) were stained with BODIPY493/503 in stationary phase (T0) and 5 h (T5) after growth in fresh medium containing cerulenin, an inhibitor of FA synthesis (Inokoshi et al., 1994). BODIPY493/503-fluorescence intensity, representing LD content, was analyzed by using flow cytometry. Consistent with previous results (Markgraf et al., 2014), LDs were utilized within 5 h of growth in wild-type cells. In contrast, LD BODIPY493/503-fluorescence persisted in *tgl3*Δ cells (Fig. S1A). Importantly, the measured fluorescence intensities and, thus, resulting LD breakdown kinetics were stable over five days (Fig. S1B). As expected, LD consumption was decreased in mutant cells lacking the functional coupling protein Ice2p or the DAG-converting enzyme Dgk1p (Fig. S1C).

To identify genes that regulate LD dynamics by mediating functional coupling to other organelles during growth resumption, we implemented a genome-wide screen in *S. cerevisiae*. A haploid non-essential knockout (KO) collection was analyzed using the newly established high throughput flow cytometry approach (Fig. 1A). The data analysis of LD content only at stationary phase revealed several mutants with high fat content that had previously been described to alter LD dynamics (Fig. S1D, Table S3). However, our results complement previous screens by identifying additional mutants with increased fat content in stationary phase (Fig. S1D, Table S3).

As shown in Fig. 1B, measurements of LD consumption in wild-type and *tgl3*Δ control cells were highly reproducible throughout the experiments. Furthermore, the global screening revealed many open reading frames (ORFs) that had previously been described to affect LD dynamics (Fig. 1C), demonstrating the feasibility of this approach (Bouchez et al., 2015; Fakas et al., 2011).

The analyzed deletion mutants were ranked according to their effect on LD consumption after correction for fat content in stationary phase and plate-to-plate assay variation. To identify cellular components and processes that are required for LD consumption during growth resumption, we analyzed the enrichment of specific gene ontology (GO) terms (namely the GO Component and the Go Process; Fig. 1D,E). We observed a strong enrichment of the complex comprising Swi3p, Snf6p and Snf2p (SWI/SNF-complex) (Fig. 1D,F) – a chromatin remodeling complex required for the enhancement of transcription by many transcription factors – among candidates that alter LD consumption kinetics. Similarly, the transcriptional regulators of phospholipid biosynthesis Ino2p and Ino4p were required for efficient utilization of LDs (transcription from RNA polymerase II promotor) (Fig. 1E,G). Strikingly, GO analysis revealed that endosomal sorting complexes required for transport (ESCRT) complexes and the vacuolar ATPase (V-ATPase) affect the dynamics of LDs during growth resumption (Fig. 1D,E).

### The ESCRT machinery is required for efficient utilization of LDs during growth resumption

We observed an enrichment of ESCRT complexes in both GO-term enrichment analyses. ESCRT proteins were specifically associated with the GO Component terms ‘ESCRT complex’, ‘ESCRT I’, ‘ESCRT II’ and ‘ESCRT III’ (Fig. 1D) and with the GO Process terms ‘ATP export’, ‘ubiquitin (Ub)-catabolic process via MVB pathway’ and ‘intraluminal vesicle formation’ (Fig. 1E). The ESCRT complexes are required for transporting cargo to the vacuole. They sequentially assemble on late endosomes, ultimately driving the formation of intraluminal vesicles and generating multivesicular bodies (MVBs). Upon fusion with the vacuole, cargo-containing intraluminal vesicles are released into the vacuolar lumen for degradation. Membrane proteins, embedded into the outer MVB membrane reach the vacuolar membrane after fusion with the vacuole (Henne et al., 2011). The deletion of ESCRT proteins leads to aberrant late endosomal structures, the Class E compartment, and a block in cargo sorting to the vacuole. ESCRT mutants are classified as class E vacuolar protein sorting (*vps*) mutants (Raymond et al., 1992).

To determine whether the ESCRT complexes are, indeed, required for LD consumption, we carried out flow cytometry experiments to test individual mutants of ESCRT complexes 0 (*vps27*Δ), I (*vps28*Δ), II (*vps25*Δ), and III (*vps20*Δ, *snf7*Δ), and Vps4p (*vps4*Δ), an AAA-ATPase required for disassembly of the ESCRT machinery. As shown in Fig. 2A, deletion mutants of all ESCRT complexes affected LD consumption. These results were confirmed by fluorescence microscopy experiments showing that BODIPY493/503-labeled LDs were rapidly consumed in wild-type cells, whereas they persisted in *snf7*Δ, *vps4*Δ and *vps20*Δ mutants (Fig. 2B). Defective LD consumption in these mutants could be due to reduced levels of Tgl3p. We, therefore, tested Tgl3p protein expression levels in stationary phase and 2.5 h after dilution into fresh medium containing cerulenin. As shown in Fig. S2A, Tgl3p expression was not altered in *snf7*Δ mutant cells when compared to wild-type cells. Furthermore, whereas overexpression of Tgl3p restored LD consumption to wild-type levels in *tgl3*Δ mutant cells, no effect of Tgl3p overexpression on LD utilization was observed in cells lacking Vps4p or Snf7p (Fig. S2B,C). These results suggest that lipolytic capacity per se is not limiting in ESCRT mutant cells.

The MVB pathway was reported to ensure cell survival during starvation (Müller et al., 2015). To exclude that the observed effects on LD consumption were caused by defects occurring during growth to stationary phase prior to initiation of growth resumption, we performed experiments using a temperature-sensitive (ts) vps4_ts mutant (Dimaano et al., 2008). Wild-type, *tgl3*Δ mutant cells and cells expressing Vps4_ts were grown to stationary phase at permissive temperature, followed by growth resumption in fresh medium containing cerulenin at non-permissive temperature. The block of Vps4p function, specifically during growth resumption, led to a significant decrease in LD consumption, whereas no effects were observed in wild-type and *tgl3*Δ mutant cells at non-permissive temperature (Fig. 2C). These data strongly indicate that

Journal of Cell Science (2018) 131, jcs213876. doi:10.1242/jcs.213876

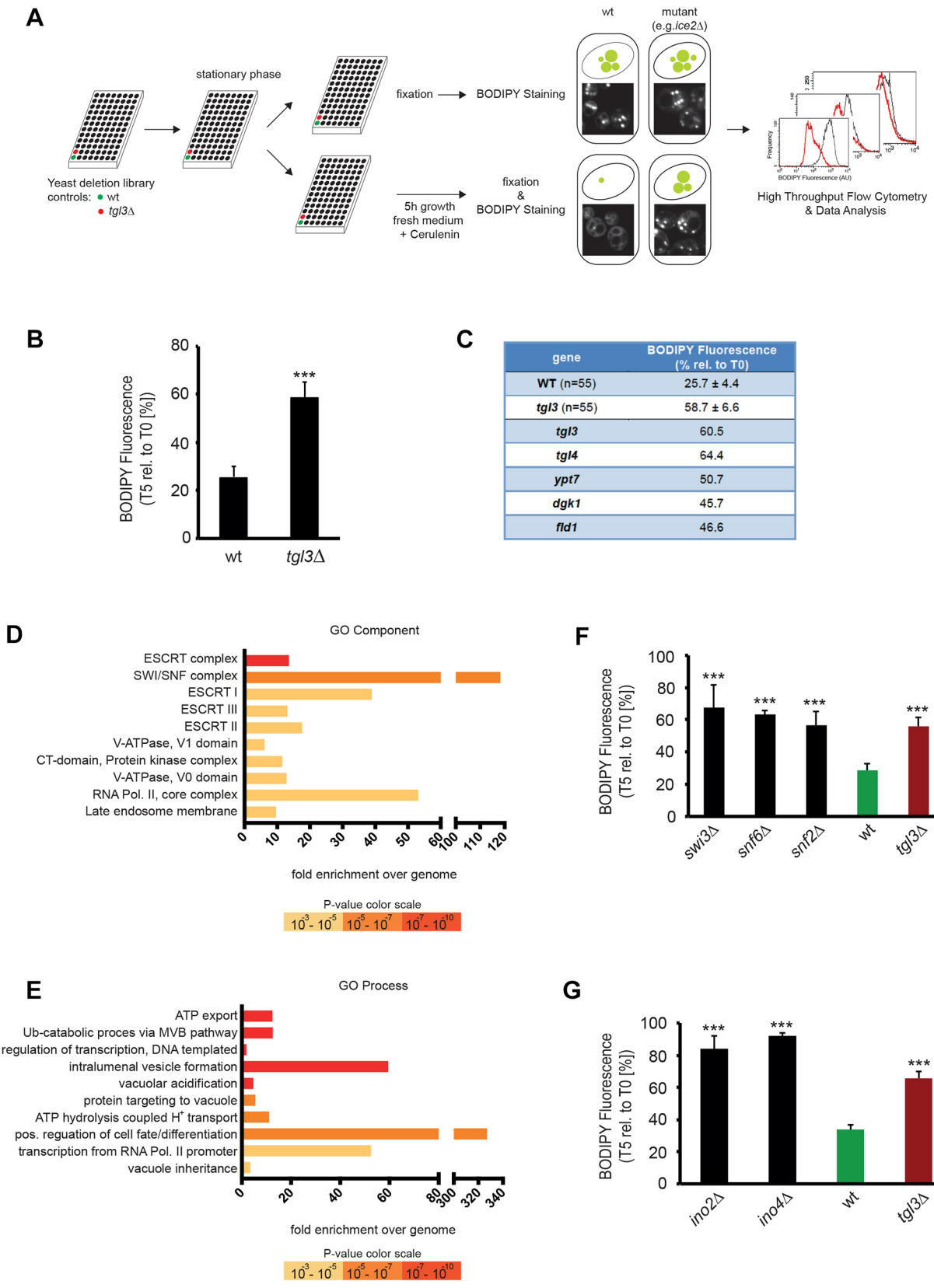


**Fig. 1.** See next page for legend.

ESCRT complexes and Vps4p, independently of their function to maintain viability during stationary phase, affect LD dynamics during growth resumption.

Consistent with a defect in lipid utilization during growth resumption, cells lacking ESCRT proteins grow slower than wild-type cells. In particular, we observed an extended lag-phase after

**Fig. 1. A genome-wide screen in *S. cerevisiae* for regulators of LD dynamics.** (A) Schematic illustration of the workflow. (B) Reproducibility of LD consumption measurements in WT and *tgl3*Δ mutant cells over 55 96-well plates, analyzed in the genome-wide screen. The LD BODIPY493/503-fluorescence at stationary phase (T0) and after 5 h growth in fresh medium containing cerulenin (T5) was measured. BODIPY493/503-fluorescence at T5 relative to T0 (in %) is shown as mean±s.d. ($n$=55). (C) Table of selected deletion mutants with known effect on LD dynamics, detected in the genome-wide screen. BODIPY493/503-fluorescence at T5 relative to T0 (in %) is shown for plate quality control samples (WT, *tgl3*Δ; $n$=55) and selected mutants. (D) GO term enrichment analysis. GO Component terms with strongest enrichment are shown, ranked in significance from top to bottom. (E) GO Process term enrichment analysis; data shown as in D. Ub, Ubiquitin. (F) The SWI/SNF complex regulates LD dynamics. LD consumption was analyzed in the indicated mutant and wt (control) strains ($n$=4–10), as described for B. (G) Ino2p and Ino4p are required for efficient utilization of LDs. Mobilization of LDs was analyzed in the indicated mutant and wt (control) strains ($n$=4–5), as described for B. Data are presented as mean±s.d.; ***$P$<0.001 versus WT.

dilution of stationary phase cells into fresh medium (Fig. 2D). Taken together, these results suggest that the ESCRT machinery is required for efficient consumption of LDs during growth resumption.

## ESCRT mediates TAG consumption for PA and phospholipid synthesis

To further understand how ESCRTs regulate LD dynamics, we diluted stationary phase cells for 5 h into fresh medium containing cerulenin and performed quantitative lipid mass spectrometry experiments at both time points, i.e. at stationary phase (T0) and 5 h after dilution (T5). In wild-type cells, TAG and DAG levels were reduced after 5 h of growth, whereas an increase in PA, PE and PI was observed (Fig. 3A-G). As expected, TAG levels remained high and no increase in phospholipid levels were observed in cells lacking Tgl3p. Consistent with our previous results (Fig. 2A,B), TAG degradation was severely delayed in *vps4*Δ cells. In contrast to wild-type and *tgl3*Δ cells, DAG levels increased after 5 h of growth, whereas phospholipid levels did not change. Interestingly, in *vps4*Δ mutants, PA levels were already lower in stationary phase and stayed low after 5 h of growth (Fig. 3C). Together, these results indicate that ESCRT is required for utilization of LD-derived DAG for PA and downstream phospholipid synthesis.

## The vacuolar ATPase is required for LD utilization during growth resumption

In addition to ESCRT complexes, GO-enrichment analysis suggested that V-ATPase mutants have a strong effect on LD dynamics during growth resumption (Fig. 1D: V-ATPase, V1/V0 domain; Fig. 1E: Vacuolar acidification, ATP hydrolysis-coupled $H^+$ transport). Yeast V-ATPase consists of 13 subunits arranged in two main domains, the membrane peripheral catalytic V1 subcomplex and the integral proton-translocating V0 complex. It functions to acidify the vacuole lumen by ATP hydrolysis-driven proton translocation across the vacuolar membrane (Forgac, 2007), thereby contributing to overall vacuole function and homeostasis (Kane, 2006; Sorensen et al., 1994; Yamashiro et al., 1990).

We next tested whether both V-ATPase subcomplexes, V0 and V1, are required for LD consumption, by analyzing vacuolar membrane ATPase (*vma*) mutants of all individual V-ATPase subunits in the flow cytometry-based assay. As shown in Fig. 4A, nearly all subunits of both subcomplexes were required for efficient utilization of LDs. These results were confirmed by fluorescence microscopy experiments showing that BODIPY493/503-labeled LDs were rapidly consumed in wild-type cells, whereas they persisted in *vma16*Δ mutants (Fig. 4C). In addition, we show that proteins involved in the assembly of the V-ATPase, such Vph2p and Vma2p, were required for LD consumption (Fig. S2D). The deletion of individual vacuolar hydrolases did not affect LD consumption kinetics (Fig. 5B). To exclude that the observed effects on LD consumption in *vma* mutant cells are due to reduced levels of the lipase Tgl3p, we analyzed its expression in cells grown to stationary phase and 2.5 h after dilution into fresh medium containing cerulenin. The levels of Tgl3p were not altered in cells lacking Vma16p or Vma5p when compared to wild-type cells (Fig. S2A). Consistent with these results, overexpression of Tgl3p did not rescue LD consumption defects in *vma16*Δ and *vma5*Δ mutant cells (Fig. S2B,C), strongly suggesting that the main lipase Tgl3p is not limiting LD utilization in cells that lack a functional V-ATPase.

Our results suggest that the defects observed in *vma* mutants result from the loss of acidification of the vacuolar lumen. To verify this hypothesis, wild-type cells were grown to stationary phase and diluted into fresh medium containing cerulenin in the presence or absence of concanamycin A, an inhibitor of V-ATPase activity (Drose and Altendorf, 1997). LD content in stationary phase and 5 h after growth resumption was analyzed by flow cytometry. The inhibition of V-ATPase activity decreased the utilization of LDs during growth resumption (Fig. 4B), confirming that altered LD dynamics in *vma* mutants results from loss of luminal acidification and vacuole function.

The deletion of V-ATPase subunits increases vacuolar pH and was shown to reduce cytosolic pH ($pH_c$) from neutral pH to pH 5.6–6.6 (Martínez-Muñoz and Kane, 2008; Young et al., 2010). Hence, we aimed to investigate whether LD utilization is affected by changes in $pH_c$ and, therefore, could explain our results in V-ATPase mutant cells. We took advantage of a hypomorphic allele of the plasma membrane ATPase Pma1p (*pma1-007*) that reduces levels and activity by 50% and, thus, renders cells unable to maintain pH homeostasis upon acidification of the culture medium. Reducing medium pH from 5 to 3 results in a decrease of $pH_c$ from 7 to 6.8 (Orij et al., 2012; Porat et al., 2005; Young et al., 2010). Wild-type, *tgl3*Δ and *pma1-007* mutant cells were grown to stationary phase in medium at pH 5.5, diluted into fresh medium at different pH values (pH 7, pH 5.5, pH 4, pH 3) containing cerulenin, and LD consumption was analyzed using the flow-cytometry-based assay. Whereas utilization of LDs was only modestly affected upon acidification of the medium in wild-type cells, a strong reduction in LD consumption was observed in *pma1-007* mutant cells (Fig. S2E). Notably, the observed effect was stronger than in any *vma* mutant we analyzed or upon addition of concanamycin A (Fig. 4A,B), despite even lower $pH_c$ had been reported in these V-ATPase-deficient cells (Martínez-Muñoz and Kane, 2008; Young et al., 2010). We, therefore, consider it unlikely that the defects in LD consumption in *vma* mutant cells are mediated by altered $pH_c$. It should be noted that, except for *vma3*Δ mutant cells, a recent genome-wide analysis of intracellular pH revealed no significant reduction in the $pH_c$ of the *vma* and ESCRT mutant cells analyzed here (Orij et al., 2012). Moreover, mutants with the strongest effect on $pH_c$, as reported by Orij et al., only showed a moderate yet not-consistent effect in our flow-cytometry assay (Fig. S2F), suggesting that the $pH_c$ value is not the underlying factor affecting LD utilization.

Sorting of the V-ATPase to the vacuole is blocked in the Class E compartment in ESCRT deletion mutants (see above; Coonrod and Stevens, 2010; Raymond et al., 1992). We, therefore, considered it likely that the effect on LD dynamics as seen in ESCRT mutants, is

Journal of Cell Science (2018) 131, jcs213876. doi:10.1242/jcs.213876

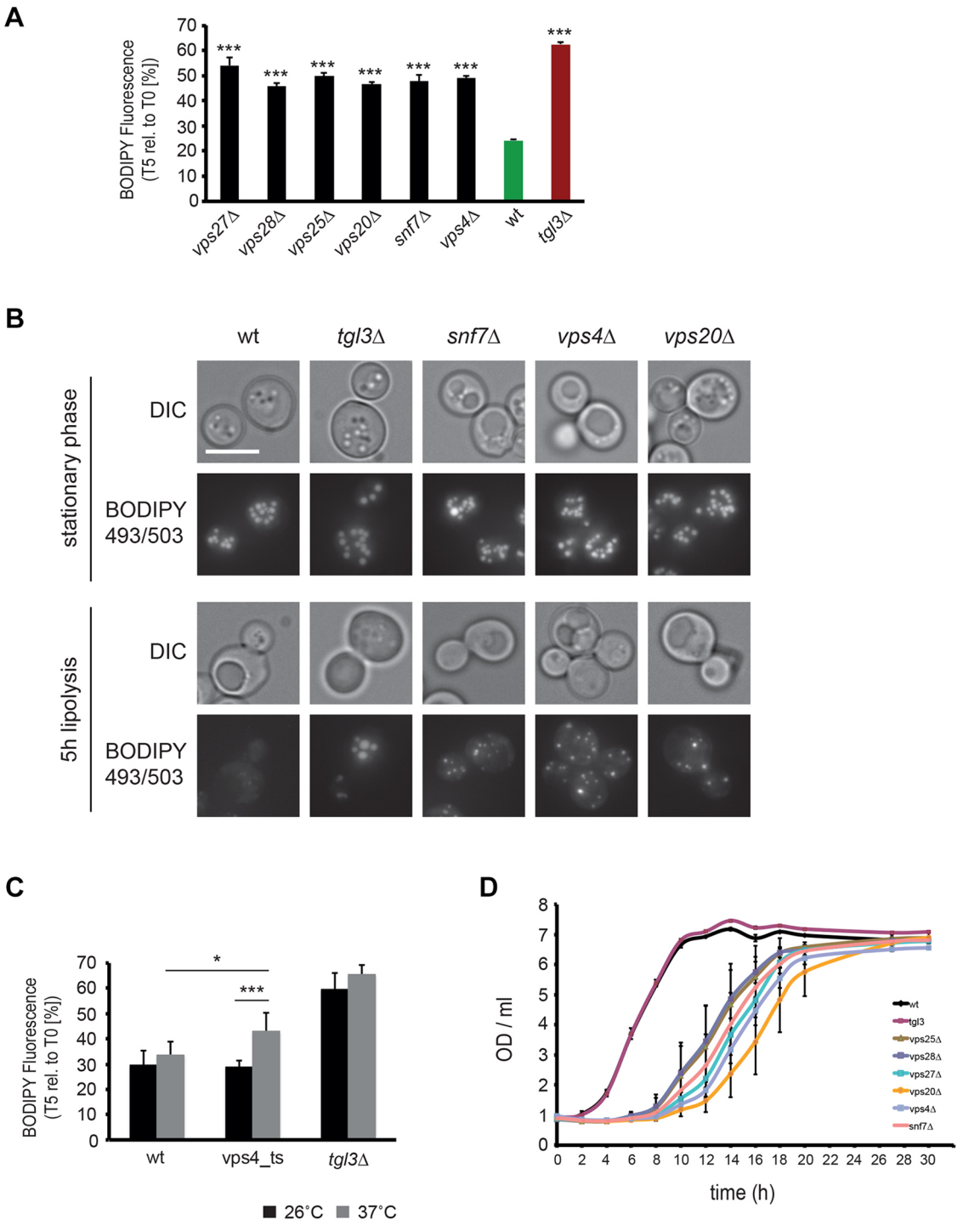


**Fig. 2. ESCRT complexes are required for efficient consumption of LDs.** (A) LD consumption was analyzed in the indicated ESCRT 0 (*vps27*Δ), I (*vps28*Δ), II (*vps25*Δ), III (*vps20*Δ and *snf7*Δ) and Vps4p (*vps4*Δ) mutant and control (wt and *tgl3*Δ) strains, as described for Fig. 1B (*n*=3). (B) Consumption of LDs in WT and indicated mutant cells after dilution from stationary phase into fresh medium was followed by BODIPY493/503 staining and fluorescence microscopy. Scale bar: 5 µm. (C) WT and *tgl3*Δ mutant cells carrying empty vector, and *vps4*Δ mutant cells carrying a temperature-sensitive mutant vps4_ts were grown to stationary phase at permissive temperature (26°C) in SC medium lacking leucine. After 30 min pre-incubation at 37°C, cells were diluted into fresh medium containing cerulenin for 5 h at 37°C. LD consumption was analyzed as in Fig. 1B (WT, *tgl3*Δ *n*=6; vps4_ts 6 clones, *n*=6 each). (D) WT and the indicated mutant cells in stationary phase were diluted into fresh medium and their growth was followed by measuring OD (*n*=3). Data are presented as mean±s.d. ***$P$<0.001 versus WT (A); *$P$<0.05 versus WT 37°C and ***$P$<0.001 versus vps4_ts 26°C (C).

mainly caused by an indirect effect on overall vacuole homeostasis. Accordingly, one would expect a similar effect on LD dynamics in vacuole protein sorting (*vps*) mutants, in particular in those, involved in late endosomal sorting. To directly test whether functional late endosome-to-vacuole protein sorting is coupled to LD dynamics, we analyzed LD utilization during growth resumption in *vps* mutants. These mutants can be grouped into Classes A–E, based on vacuole morphology (Bowers and Stevens,

Journal of Cell Science (2018) 131, jcs213876. doi:10.1242/jcs.213876

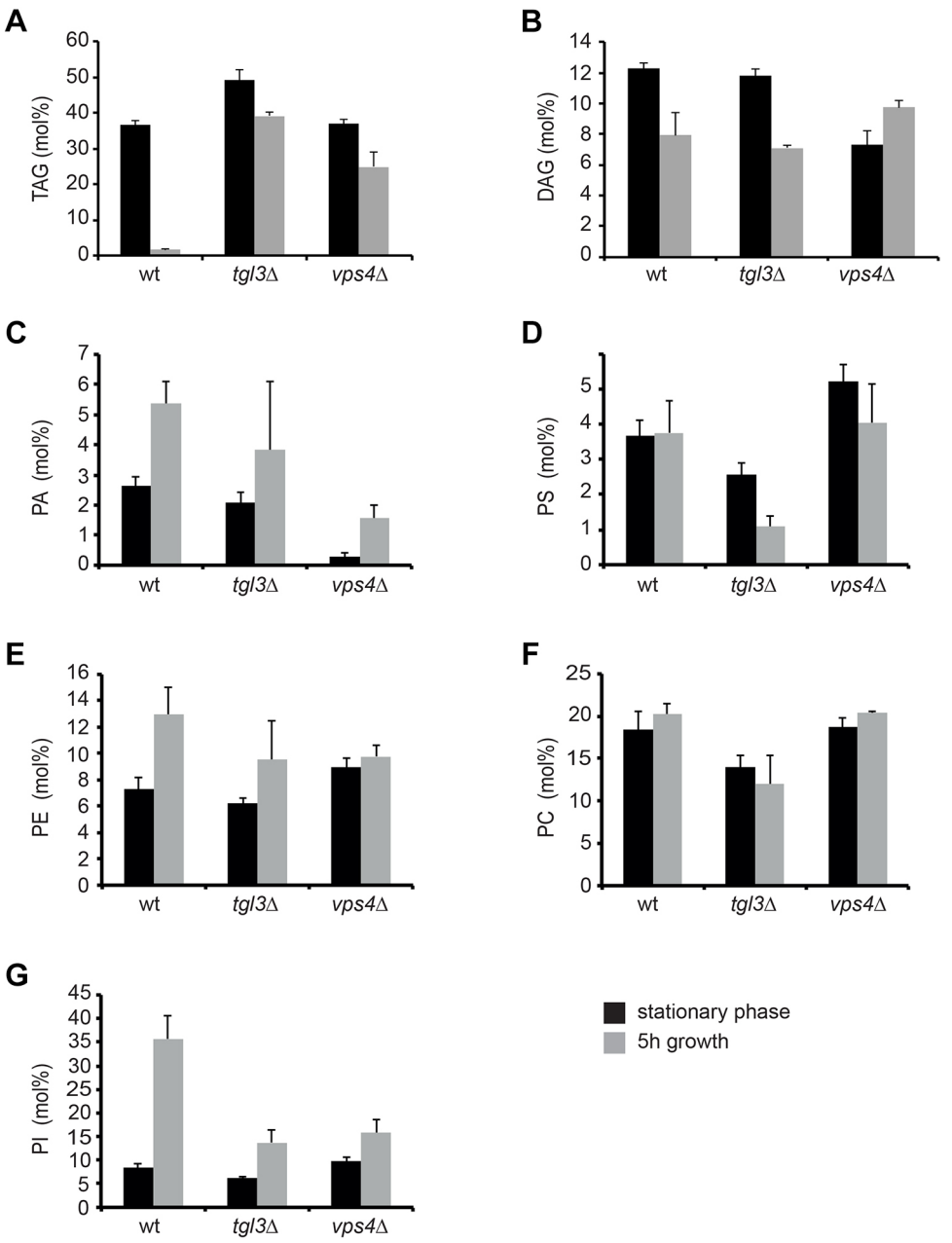


**Fig. 3. Lipid mass spectrometry analysis of WT, *tgl3*Δ and *vps4*Δ mutant cells.** (A–F) The lipid composition of WT, *tgl3*Δ and *vps4*Δ cells was analyzed in stationary phase and 5 h after dilution into fresh medium containing cerulenin. The indicated lipid species (TAG, triacylglycerols; DAG, diacylglycerol; PA, phosphatidic acid; PS, phosphatidylserine; PE, phosphatidylthanolamine; PC, phosphatidylcholine; PI, phosphatidylinositol) were analyzed by quantitative mass spectrometry. Data from two independent experiments were analyzed in duplicates and are shown as mean+s.d.

2005; Raymond et al., 1992). Our results reveal that LD consumption during growth resumption is affected in some Class B mutants (small fragmented vacuoles; *vps41*Δ, *vps17*Δ, *vps43*Δ) and specifically in late endosomal Class D mutants (single large vacuole; *vps15*Δ, *vps3*Δ, *vps6*Δ, vps45Δ; Fig. 4D). Our results, therefore, suggest that LD dynamics during growth resumption are coupled to vacuole homeostasis.

### LD utilization during growth resumption is not mediated by autophagy

LDs have been shown to be degraded in the vacuole via microautophagy in stationary phase and upon nitrogen starvation, requiring the core autophagy machinery (van Zutphen et al., 2014; Wang et al., 2014). In contrast, microautophagy after a diauxic shift does not require the autophagy machinery but the vacuolar lipase Atg15p, proteinase A (Pep4p) and ESCRT complexes (Oku et al., 2017). Microautophagy has not been described to occur during growth resumption. However, to specifically test whether microautophagy contributes to LD utilization during growth resumption, we analyzed LD consumption in autophagy mutant cells using the flow cytometry approach. The deletion of autophagy-related genes (*atg*) did not affect utilization of LDs (Fig. 5A). Importantly, neither the vacuolar lipase Atg15p nor proteinase A (Pep4p), both of which are implicated in ESCRT-dependent microautophagy after diauxic shift, were required for LD utilization during growth resumption (Fig. 5A,B). To directly probe for LD uptake into vacuoles during growth resumption, we followed BODIPY493/503-labeled LDs and FM4-64-labeled vacuoles by fluorescence microscopy 2 h after diluting cells from stationary phase into fresh medium containing cerulenin. As shown in Fig. 5C, LDs were often found in close proximity to vacuoles. However, uptake of LDs into FM4-64-labeled vacuoles was negligible. Similar results were obtained when LD autophagy was analyzed in cells

Journal of Cell Science (2018) 131, jcs213876. doi:10.1242/jcs.213876

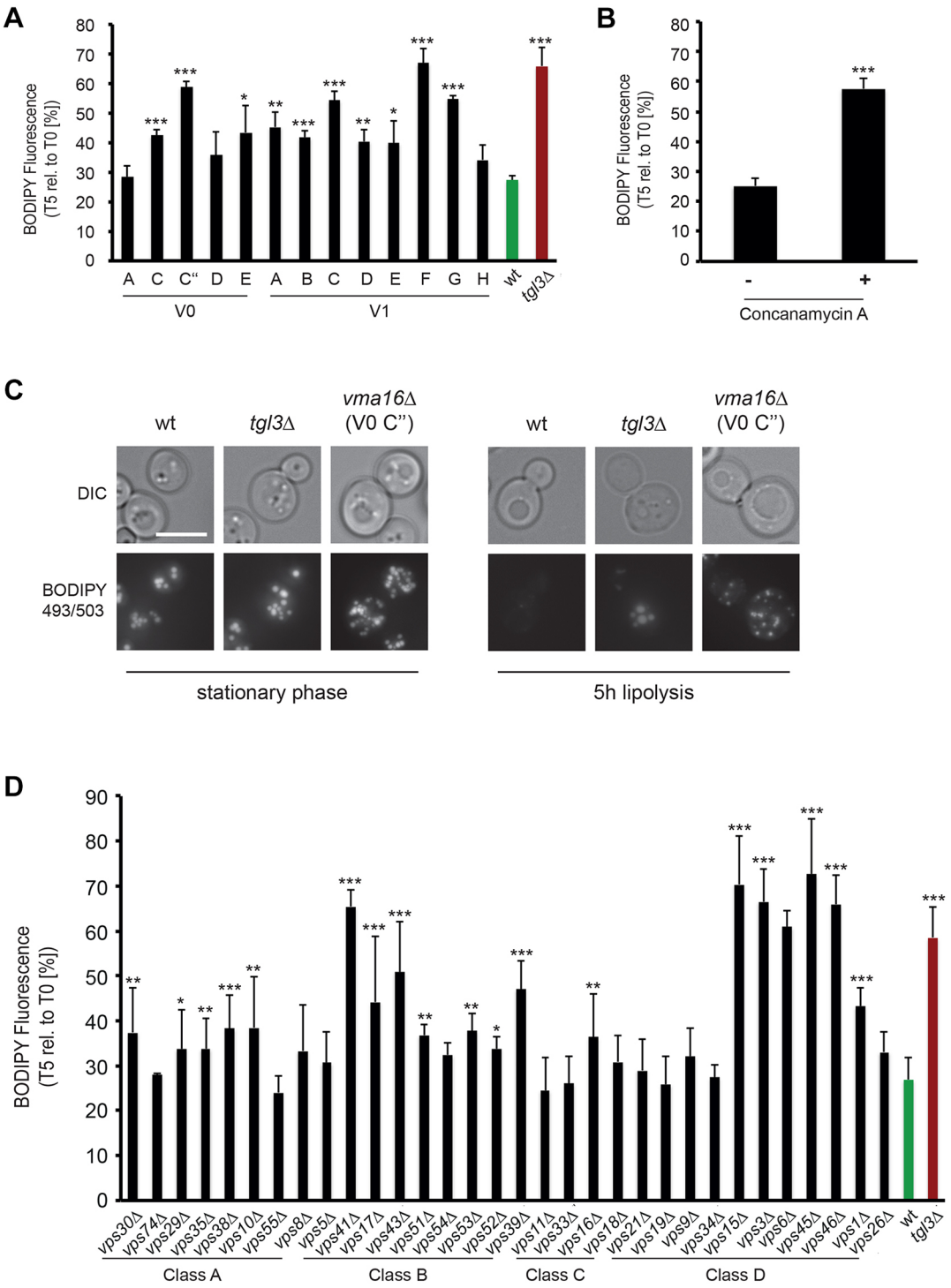


**Fig. 4. V-ATPase and proteins involved in late endosomal protein sorting are required for efficient utilization of LDs during growth resumption.** (A) LD consumption was analyzed in the indicated V-ATPase mutant (domain V0/V1, subunits A-H) and control strains ($n$=4), as described for Fig. 1B. (B) Analysis of LD consumption as shown in A but the consumption of BODIPY493/503-labeled LDs was followed in cells diluted into fresh medium with either DMSO as a control (–) or 100 ng/ml concanamycin A (+); ($n$=4). (C) Consumption of LDs in wild-type (wt), control (*tgl3*Δ) and *vma16*Δ mutant cells (V0 SU c'' vma16Δ) after dilution from stationary phase into fresh medium containing 10 µg/ml cerulenin was followed by BODIPY493/503 staining and fluorescence microscopy. Scale bar: 5 µm. (D) Analysis of LD consumption carried out as described in A but in vacuolar protein sorting (*vps*) mutant strains (grouped according to vacuole morphology phenotype, i.e. Class A–D) as indicated, and wild-type (wt) and control (*tgl3*Δ) ($n$=7). Data are presented as mean+s.d.; *$P$<0.05, **$P$<0.01, ***$P$<0.001 versus WT (A,D); ***$P$<0.001 versus control (B).

expressing the LD marker protein Erg6p fused to GFP (Erg6p-GFP; Fig. S3A). Together, these results strongly suggest that LD utilization during growth resumption occurs independently of LD-autophagy (lipophagy). The observed defects on LD dynamics in the identified ESCRT-, V-ATPase and *vps* mutant cells are, therefore, mediated by a lipophagy-independent process.

Journal of Cell Science (2018) 131, jcs213876. doi:10.1242/jcs.213876

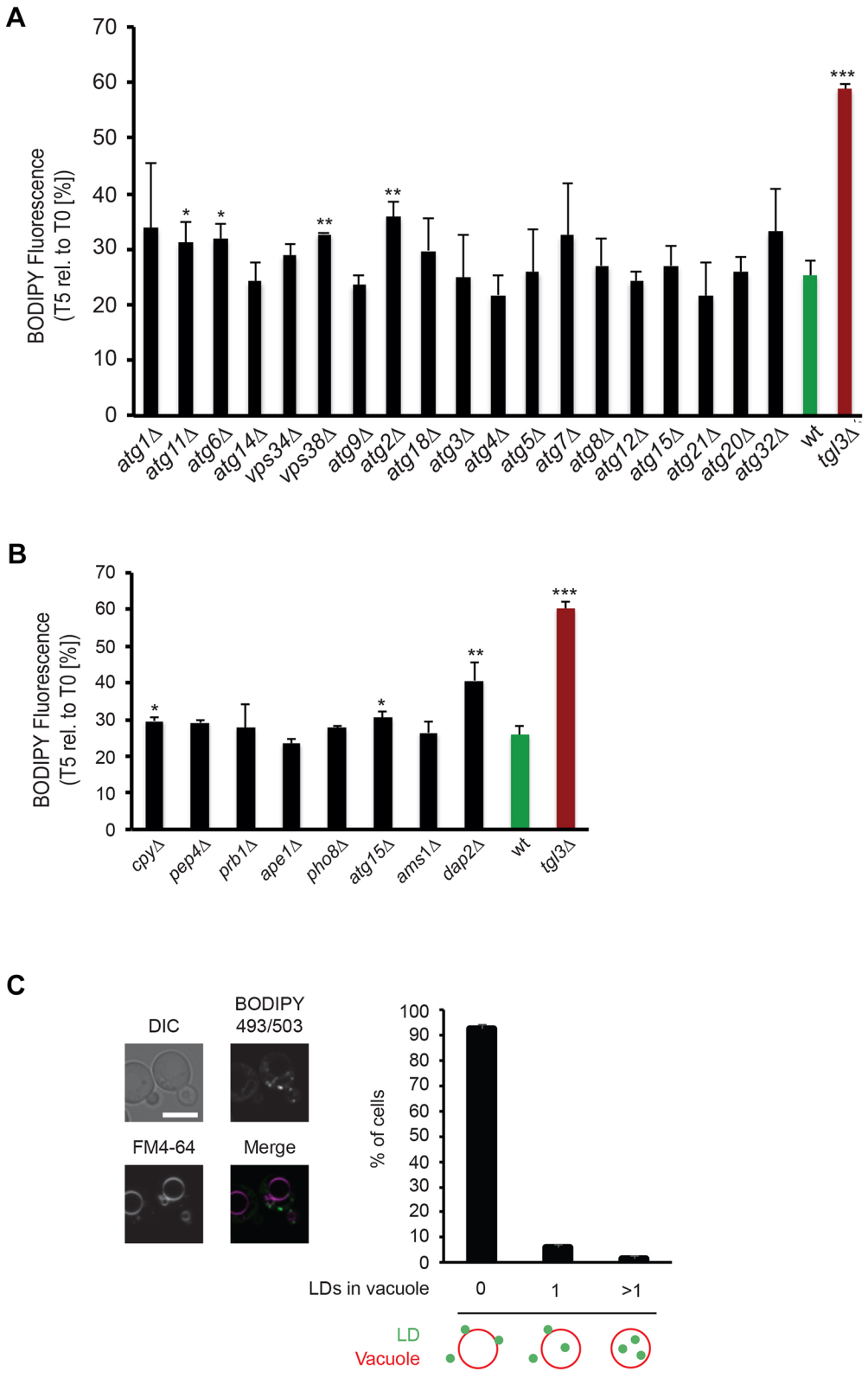


**Fig. 5. LD utilization during growth resumption is not mediated via autophagy.** (A) LD consumption was analyzed in the indicated autophagy-related gene (*atg*) mutants ($n$=4), as described in Fig. 1B. (B) Analysis of LD consumption as shown in A, but in the indicated mutants, and compared with wild type (wt) and control (*tgl3*Δ) ($n$=4). (C) LD autophagy during growth resumption. Cells were diluted from stationary phase and diluted into fresh medium containing cerulenin for 2 h. BODIPY493/503-labeled LDs and vacuoles stained with FM4-64 were analyzed by fluorescence microscopy. For the quantification of LD autophagy, eight randomly chosen microscopy images were analyzed ($n$=1011 cells). Scale bar: 5 µm. Data are presented as mean±s.d.; *$P$<0.05, **$P$<0.01, ***$P$<0.001, versus WT (A,B).

### TORC1 signaling from functional vacuoles is required for LD consumption

Vacuoles are highly dynamic organelles, undergoing coordinated membrane fusion and fission reactions throughout the cell cycle and in response to changes in environmental conditions. Target of rapamycin complex 1 (TORC1) presents the main signaling hub, sensing vacuole status and communicating it to the cell-cycle machinery (Jin and Weisman, 2015). TORC1 signals through two effector proteins, Sch9p or Sit4p, to regulate downstream transcription factors and can be specifically inhibited by rapamycin (De Virgilio and Loewith, 2006; Di Como and Arndt, 1996; Heitman et al., 1991; Jacinto et al., 2004; Loewith et al., 2002; Urban et al., 2007).

Journal of Cell Science (2018) 131, jcs213876. doi:10.1242/jcs.213876

Based on our results showing that LD dynamics are coupled to vacuole homeostasis, we asked whether TORC1 is involved in regulating LD consumption in response to vacuole status. Initial evidence for the interplay between TORC1 and LDs came from a study showing that inhibition of TORC1 by rapamycin induces LD synthesis (Madeira et al., 2015). Furthermore, TORC1 was shown to inhibit phosphatidic acid hydrolases, key regulators of membrane- and storage lipid synthesis, in yeast and mammals (Pah1p and lipid-1, respectively) (Dubots et al., 2014; Eaton et al., 2013; Lamming and Sabatini, 2013; Peterson et al., 2011). These complementary data indicate that defects in vacuole homeostasis, as observed in e.g. ESCRT mutant cells, could be sensed by TORC1 and transduced to the LD machinery. According to this model, TORC1 signaling from functional vacuoles could inhibit Pah1p activity, ultimately directing LD-derived DAG into membrane lipid biosynthesis pathway. In contrast, defects in vacuole status would inhibit TORC1 signaling and could de-repress Pah1p activity, increase DAG:PA ratios and, thus, prevent LD and DAG utilization during growth resumption.

These assumptions were supported by several experiments. First, we analyzed LD consumption in the presence of rapamycin. As shown in Fig. 6A, addition of rapamycin inhibited LD utilization during growth resumption in wild-type cells. Importantly, this effect is not due to reduced expression levels of Tgl3p – which were comparable in the presence or absence of rapamycin during growth resumption (Fig. S3B). Consistent with TORC1 signaling affecting DAG-to-PA conversion downstream of TAG hydrolysis, we did not see an additional effect of rapamycin on LD consumption in cells lacking Tgl3p. Second, by using a targeted lipidomics approach we show that addition of rapamycin inhibits utilization of DAGs during growth resumption (Fig. 6B), similar to cells lacking Vps4p (Fig. 3B). This, furthermore, supports the hypothesis that Tgl3p lipolytic activity is not limiting during rapamycin treatment but provides TAG-derived DAG that cannot be further utilized. In contrast, the complete block of Tgl3p activity does not affect utilization of DAGs during growth resumption (Fig. 3B). Third, LD consumption requires the TORC1 effector protein Sit4p but not Sch9p (Fig. 6C). Next, we tested whether rapamycin affects LD consumption in ESCRT mutant cells. As shown in Fig. 6D, no additional effect of rapamycin on LD dynamics was observed in cells lacking Vps4p. This result suggests that TORC1 signaling is defective in *vps4*Δ mutant cells and can, thus, not be further inhibited by rapamycin. To directly assess the activity of TORC1 in cells that lack a functional ESCRT machinery, we conducted a rapamycin recovery assay (Dubouloz et al., 2005; Takeda et al., 2018). As expected, cells lacking the TORC1 subunit Tco89p were highly sensitive to rapamycin. Importantly, *snf7*Δ and *vps4*Δ mutant cells exhibited increased sensitivity to rapamycin, indicating that TORC1 signaling is, indeed, attenuated in these mutants (Fig. 6E).

If defective TORC1 signaling in *vps4*Δ mutant cells would be transduced to the LD machinery by inhibiting the DAG-to-PA conversion, DAG:PA ratios in these mutant cells would be increased. This assumption was confirmed by lipidomics experiments showing that DAG:PA ratios are higher in *vps4*Δ cells compared to wild-type cells, in stationary phase and after 5 h lipolysis during growth resumption (Fig. 6F). It should be noted that the defect in LD consumption could not be rescued by supplementation with inositol (Fig. S3C), a compound that stimulates PI synthesis by utilizing PA and shifts the balance towards the CDP-DAG pathway when substrates are spatially accessible to the respective enzymes Cds1p and Pis1p in the ER. In summary, the data presented here support a model in which vacuole functionality is signaled to the LD catabolic machinery during growth resumption through TORC1-mediated regulation of enzymes that are involved in DAG-PA interconversion.

Besides the unidirectional communication described above, these data have implications for a bidirectional crosstalk between both organelles. Vacuole dynamics are balanced by fusion and fission reactions that require a specific set of proteins and lipids, i.e. DAG and PA (Miner et al., 2017; Sasser et al., 2012; Wickner, 2010). Altered TORC1 signaling from impaired vacuoles towards the LD catabolic machinery as described here, therefore, results in a feedback loop that ultimately affects vacuole dynamics through changes in the levels of the LD-derived DAGs and PA. Interestingly, this model suggests that DAG is channeled from LDs towards vacuoles during growth resumption. To test whether LD-derived DAG is channeled towards vacuoles, we followed DAG distribution during growth resumption by using a GFP-tagged DAG reporter (C1δ-GFP; Fig. 6G) (Ganesan et al., 2015). Consistent with experiments in cells grown to exponential phase, C1δ-GFP localizes to vacuolar structures 4 h after diluting stationary phase wild-type cells into fresh medium containing cerulenin. At this time-point, unspecific staining of the LD-marker protein Erg6p fused to RFP (Erg6p-RFP) was observed, indicating that LDs were utilized efficiently. However, in stationary phase, C1δ-GFP accumulated in punctate structures adjacent to LDs labeled with Erg6p-RFP. Similarly, C1δ-GFP localized to LD proximal sites in cells that lack Vps4p in stationary phase. However, no vacuolar localization of C1δ-GFP after 4 h of growth in fresh medium containing cerulenin was observed in *vps4*Δ mutant cells (Fig. 6G). Together, these results suggest that (i) LD-derived DAG is channeled not only into membrane lipid biosynthesis pathways in the ER but also towards the vacuole and (ii) vacuole homeostasis defects (e.g. in *vps4*Δ cells) not only alter the DAG:PA ratio but also halt the subcellular distribution of DAG towards vacuoles.

## DISCUSSION

LDs interact with a variety of cellular organelles. Our data provide detailed insight into how the dynamics of LDs and vacuoles are coordinated throughout cell growth. We developed a flow cytometry-based assay to measure LD breakdown kinetics during growth resumption and screen all non-essential deletion mutants in yeast. This screen revealed that a functional vacuole, independent of its role in autophagy, is required for efficient utilization of LDs (Fig. 7). When cells resume growth in fresh medium, TORC1 signaling from vacuoles facilitates net conversion of DAG to PA. As a result, DAG derived from TAG-hydrolysis on LDs can be converted to PA and processed in downstream lipid synthesis processes required for growth. In contrast, compromised vacuoles in, e.g. ESCRT mutant cells, inhibit TORC1 signaling, subsequently inhibiting efficient DAG-to-PA conversion and, thus, preventing the utilization of LDs and LD-derived DAG. Based on our previous results on the DAG channeling enzyme Ice2p we consider that accumulated DAGs are likely to be re-esterified to TAGs on LDs (Markgraf et al., 2014).

Specifically, we show that LD breakdown during growth resumption is defective in ESCRT-, V-ATPase- and late endosome to vacuole *vps* mutants. ESCRT complexes were shown to be required for consumption of LDs through microautophagy after diauxic shift. Whereas this process does not require the core autophagy machinery, it depends on the vacuolar lipase Atg15p and proteinase A (Pep4p) (Oku et al., 2017). Our results clarify that LD-autophagy does not contribute to LD utilization during growth resumption. Consistent with this finding,

Journal of Cell Science (2018) 131, jcs213876. doi:10.1242/jcs.213876

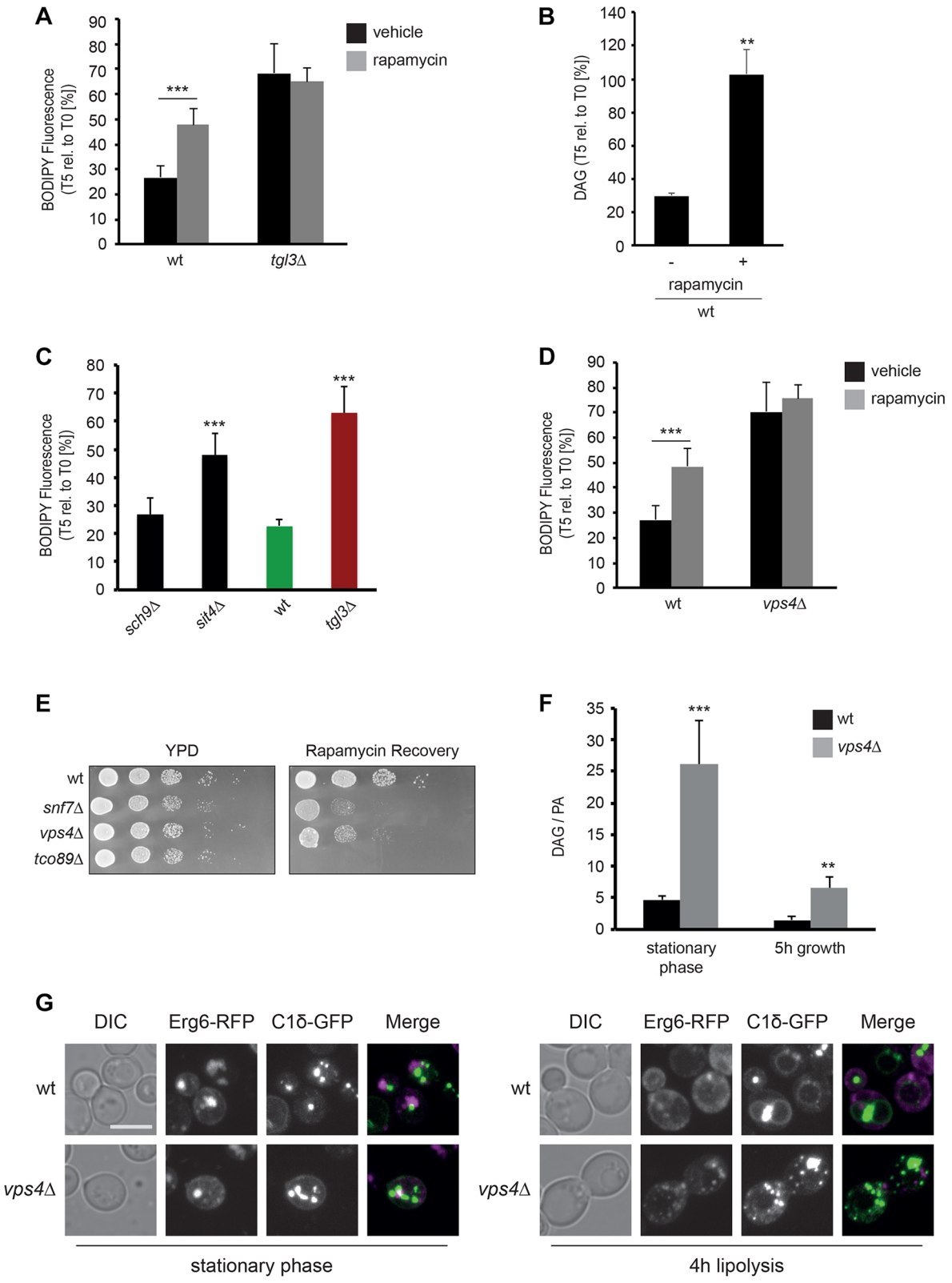


**Fig. 6.** See next page for legend.

LD breakdown depends on the LD-associated lipase Tgl3p but not Atg15p or Pep4p.

Rather than being directly involved in LD consumption, our data suggest that ESCRT complexes indirectly affect LD dynamics by regulating vacuole functionality. The ESCRT machinery is required for the formation of MVBs, cargo sorting to the vacuole and, ultimately, for maintaining vacuole homeostasis. The deletion of ESCRT proteins leads to aberrant late endosomal structures, the

Journal of Cell Science (2018) 131, jcs213876. doi:10.1242/jcs.213876

**Fig. 6. Regulation of LD consumption by TORC1 signaling and ESCRT-dependent changes in ratios and distribution of vacuole fusion-relevant lipids.** (A) LD consumption in wild-type (wt) and *tgl3*Δ cells was analyzed as described for Fig. 1B in the absence (control) or presence of rapamycin (*n*=6-8). (B) Utilization of DAG during growth resumption. WT cells were grown to stationary phase (T0) and diluted into fresh medium containing cerulenin in the presence or absence (–) of rapamycin for 5 h (T5). Levels of DAG were analyzed using a targeted lipidomics approach. DAG at T5 relative to T0 (in %) is shown (*n*=3). (C) LD consumption was analyzed as described for Fig. 1B in strains indicated (*n*=7-10). (D) LD consumption was analyzed as described for Fig. 1B in strains indicated in the absence (control) or presence of rapamycin (*n*=8). (E) Spotting assay analyzing growth recovery after rapamycin treatment in WT and the indicated mutant strains. Cells in log phase were grown in the presence or absence of rapamycin (200 ng/ml) for 3 h at 30°C. The cell cultures were serially diluted and spotted on YPD medium. Colonies were imaged after one day (YPD) or two days (rapamycin recovery). (F) Ratio of DAG to PA in WT and *vps4*Δ mutant cells. Cells were analyzed by quantitative lipid mass spectrometry in stationary phase and 5 h after dilution into fresh medium containing cerulenin. (G) The localization of DAG-Reporter (C1δ-GFP) was analyzed by fluorescence microscopy in WT and *vps4*Δ mutant cells expressing Erg6p-RFP at stationary phase and 4 h after dilution into fresh medium containing cerulenin. A maximum projection is shown. Scale bar: 5 µm. Data are presented as mean±s.d.; ***P*<0.01, ****P*<0.001, versus control (A,B,D) or WT (C,F).

Class E compartment, a block in cargo sorting to the vacuole and, thus, a non-functional vacuole. Vacuolar defects in class E mutants result, in part, from the missorting of the V-ATPase. Interestingly, we observed a strong defect in LD utilization in most V-ATPase mutants and upon inhibition of V-ATPase activity. These results contrast those from previous studies, showing that only the V1 domain affects LD dynamics, independently of V-ATPase activity (Bouchez et al., 2015). However, these experiments were conducted in exponential and early-stationary phase and, together with results presented here, suggest that correct sorting of V-ATPase and its activity are specifically required to maintain LD dynamics during growth resumption. If ESCRT mediates its effect on LD dynamics indirectly by maintaining vacuole homeostasis, one would expect additional *vps* mutants to affect LD consumption. Consistent with this hypothesis, we observed that late endosomal *vps* proteins are required for efficient LD utilization during growth resumption.

How is the vacuolar status sensed and signaled to LDs? Previous studies have shown that a defective vacuolar system caused by, e.g. vacuole inheritance defects, is sensed and signaled to the cell cycle machinery via TORC1 and its effector Sch9p (Jin and Weisman, 2015). A direct regulatory link between TORC1 signaling and LD dynamics was established in studies showing that TORC1 activity phosphorylates and inhibits PA hydrolase Pah1p, in part via the Nem1–Spo7 complex (Dubots et al., 2014). Vacuolar status can then be sensed and signaled to LDs through TORC1-mediated regulation of Pah1p. Vacuolar defects would result in diminished TORC1 signaling, de-repression of Pah1 and increased DAG:PA ratios, ultimately blocking utilization of LDs and LD-derived DAGs. Consistent with this model, we show that: (i) LD utilization during growth resumption requires TORC1 signaling involving the effector phosphatase Sit4p, (ii) inhibition of TORC1 signaling during growth resumption leads to accumulation of DAG, (iii) LD consumption in Vps4p mutant cells is insensitive to TORC1 inhibition owing to inherent TORC1-signaling defects that are probably the result of vacuolar dysfunction and, (iv) the DAG:PA ratio increases in Vps4p mutant cells.

Despite the well-established connection between TORC1 signaling and PA phosphatase activity in yeast and mammalian cells our data do not exclude that alterations in DAG and PA levels in ESCRT mutant cells are mediated through regulation of other enzymes that affect DAG:PA ratios, e.g. Dgk1p. In fact, phosphorylation of Dgk1p by casein kinase II (CKII) has recently been shown to regulate its activity and, thus, the synthesis of phosphatidic acid. However, Dgk1p-dependent growth resumption from stationary phase is not governed by the CKII-mediated phosphorylation of the enzyme (Qiu et al., 2016). Whether Dgk1p activity during growth resumption is regulated by other kinases, such as TORC1, does, therefore, need to be carefully assessed in future studies.

DAGs and PA present key lipid intermediates in the formation and consumption of LDs, and have been implicated to regulate vacuole dynamics. In fact, alterations of DAG:PA ratios by deletion of Pah1p or Dgk1p cause vacuole fragmentation or augmented fusion, respectively (Miner et al., 2017; Sasser et al., 2012). Therefore, rather than unidirectional crosstalk between vacuoles and LDs, our data suggest a bidirectional feedback-loop between both organelles. According to this model, TORC1 signaling from functional vacuoles in wild-type cells reduces DAG:PA ratios, thereby driving vacuole fragmentation, which is beneficial for the inheritance of vesicular/tubular structures to the daughter cell. Functional ESCRT complexes and TORC1 have, indeed, been shown to promote vacuole fragmentation (Michaillat et al., 2012; Michaillat and Mayer, 2013; Stauffer and Powers, 2015). In contrast, defective TORC1 signaling in mutants that affect vacuole

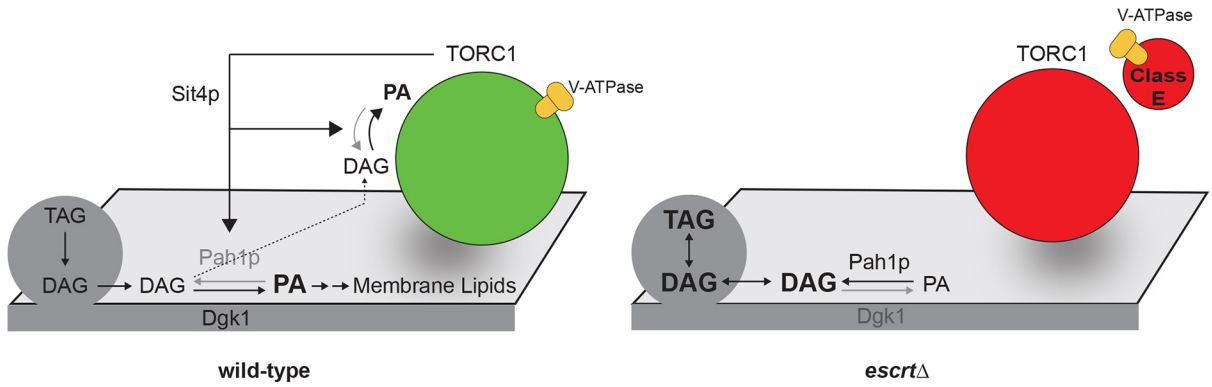


**Fig. 7. Model of functional coupling of LD and vacuole dynamics.** (Left panel) TORC1-signaling from functional vacuoles (green circle) mediates mobilization of LDs during growth resumption by regulating interconversion between DAG and PA, thus allowing efficient utilization of LD (gray circle)-derived DAG for membrane lipid biosynthesis in wild-type cells. (Right panel) Defective TORC1-signaling due to dysfunctional vacuoles (red circle) prevents the efficient utilization of LD-derived DAG for PA synthesis, as well as downstream membrane lipid synthesis in, for example, ESCRT mutant (escrtΔ) cells.

Journal of Cell Science (2018) 131, jcs213876. doi:10.1242/jcs.213876

homeostasis would affect LD breakdown kinetics by increasing DAG:PA ratios, possibly by de-repressing Pah1p, ultimately promoting vacuole fusion. Importantly, this model suggests channeling of LD-derived DAG towards vacuoles. In agreement with this notion we observe changes in the subcellular localization of a fluorescently labeled DAG-reporter from LD-proximal sites towards vacuoles during growth resumption.

It remains unclear how DAG is channeled from LD-proximal sites to the vacuole and how this process is regulated. Membrane contact sites (MCS) are implicated in transport of lipids between organelles (Helle et al., 2013; Jain and Holthuis, 2017). The nucleus–vacuole junction (NVJ) mediates physical contact between the perinuclear and vacuolar membrane, and is facilitated by a direct interaction between the vacuolar protein Vac8p and the nuclear membrane protein Nvj1p (Malia and Ungermann, 2016; Pan et al., 2000). Additional proteins contributing to NVJ formation, such as Mdm1p, have been described (Henne et al., 2015). Consistent with our observed accumulation of the DAG reporter protein C1δ-GFP at LD-proximal sites, the DAG-generating enzyme Pah1p concentrates in nuclear membrane punctae that flank the NVJ and are in contact with LDs in stationary phase, indicating a functional relationship between LDs and vacuoles at NVJs (Barbosa et al., 2015). It is, thus, tempting to speculate that LD-derived DAG is channeled towards vacuoles through NVJ during growth resumption; however, detailed studies are needed to specifically address this question.

Finally, bidirectional crosstalk between vacuoles and LDs would create a self-propagating signaling system, as studies in mammalian systems revealed that PA stabilizes and activates mammalian TORC1 (mTORC1) (Menon et al., 2017; Toschi et al., 2009; Yoon et al., 2011). Thus, TORC1 signaling from functional vacuoles in wild-type cells would allow efficient conversion of DAG to PA, which, in fact, could stabilize and enhance TORC1 activity. In contrast, diminished TORC1 signaling, as response to vacuolar dysfunction, would result in reduced PA levels that would further abolish TORC1 signaling. Such a system would ensure that even small defects in vacuolar function are communicated efficiently within the cellular organelle network, i.e. to LDs.

In summary, by implementing a genome-wide screen in yeast, we unravel a tight interplay between vacuoles and LDs during growth resumption (summarized in Fig. 7). Our data explain how the dynamics of cellular organelles are coordinated, and we present first mechanistic insight into how LDs are integrated into an overall metabolic network. Given the conserved role of LDs and vacuoles/lysosomes in cellular metabolism, the results presented here are likely to be significant for higher eukaryotic cell systems. In fact, recent studies have described that mammalian TORC1 (mTORC1) senses and signals lysosomal status, i.e. amino acid status through V-ATPase, and lysosomal cholesterol through a complex comprising the amino acid transporter SLC38A9 and the Niemann-Pick C1 (NPC1) protein (Castellano et al., 2017; Zoncu et al., 2011). In addition, it is now well-accepted that mTORC1 regulates hepatic lipid metabolism via lipin-1 and the SREBP transcriptional network (Lamming and Sabatini, 2013; Peterson et al., 2011). Direct crosstalk between lysosomes and LDs to coordinate their status and dynamics, equivalent to the mechanism described in yeast might, therefore, exist in higher eukaryotic cells. Finally, owing to the central role of LDs in metabolic disorders, it will be important to carefully examine how functional coupling of LDs and lysosomes affects such diseases, in order to develop future treatment strategies.

## MATERIALS AND METHODS

### Strains, plasmids and growth conditions

Strains used in this study are isogenic to BY4741 (Mat a ura3Δ his3Δ1 leu2Δ0 met15Δ0) and are listed in Table S1. Yeast genetic manipulations were accomplished by homologous recombination of PCR fragments. Tgl3p was genomically tagged at the C-terminus using a 3HA-HIS3 cassette amplified from pFA6a-3HA-HIS3 (Longtine et al., 1998). A deletion library of single knockouts of non-essential genes was purchased from GE Dharmacon. Plasmids used in this study are described in Table S2. To generate a plasmid overexpressing a 3HA-tagged version of Tgl3p, 3HA was amplified from pFA6a-3HA-HIS3, digested with HindIII/XhoI and ligated into the HindIII/XhoI sites of p415-ADHpr (Nguyen et al., 2012). Tgl3p was amplified from genomic DNA and, after digestion with SpeI/HindIII, it was ligated into the SpeI/HindII sites of plasmid p415-ADHpr-3HA. Cells were grown at 30°C in synthetic complete (SC) medium. SC medium contained 6.7 g/l yeast nitrogen base with ammonium sulfate (MP Biomedical), 20 g/l glucose, and was supplemented with the required amino acid mixtures (Complete Supplement Mixture [CSM] 0.79 g/l; CSM-leucine 0.69 g/l; MP Biomedical). For experiments, logarithmically grown precultures were diluted to 0.5 optical density (OD) units/ml and grown overnight to reach stationary phase. The cells were harvested by centrifugation and diluted into fresh medium to OD=1. FM4-64 was purchased from Thermo Fischer. Cerulenin, rapamycin and concanamycin A were purchased from Sigma Aldrich. Where indicated, the FA synthesis inhibitor cerulenin was added to cultures from a 10 mg/ml stock solution in ethanol to a final concentration of 10 µg/ml. The V-ATPase activity inhibitor concanamycin A (100 µM stock solution in DMSO) was added to cultures to a final concentration of 1 µM. The TORC1 signaling inhibitor rapamycin (100 µg/ml stock solution in 90% ethanol, 10% Tween-20) was adjusted to a final concentration of 100 ng/ml.

### Genome-wide screen for regulators of LD dynamics

A collection of all non-essential yeast deletion strains, stored as glycerol stocks in 55 96-well plates, was processed batch-wise. Cells were thawed and transferred to solid yeast extract peptone with 2% glucose (YPD) using a 96-pin replicator (V&P Scientific). The pin replicator was sterilized by incubating two times for 1 min in sterile water, 1 min in bleach (10% sodium hypochloride) and 1 min in ethanol (70%), followed by flame sterilization. Plates were incubated for 2 days at 30°C. Cells were transferred to 96-well plates containing SC medium, 2% glucose (150 µl/well). Wild-type and *tgl3*Δ cells were added to two empty positions on each plate to serve as controls and to evaluate assay variability and reproducibility. Precultures were incubated overnight (12 h) at 30°C with shaking. The OD was measured and cells were diluted to OD=0.5. After incubation for 24 h at 30°C with shaking, OD was measured over a period of 2 h to ensure that cells reached stationary phase. An aliquot of stationary-phase cells was transferred to a new plate, harvested by centrifugation and washed once with phosphate buffered saline (PBS; Wellwash 4MK2, Labsystems). Cells were fixed by incubation in 150 µl PBS containing 3.7% paraformaldehyde for 30 min, washed once with PBS and stored in ice-cold PBS at 4°C. A second aliquot of cells was transferred to a fresh 96-well plate and diluted into fresh SC medium containing 10 µg/ml cerulenin. The cells were incubated for 5 h at 30°C with shaking; OD before (T0) and after 5 h incubation (T5) was measured. Cells were fixed as described above. LDs in cells from stationary phase and after 5 h growth were stained with BODIPY 493/503 in PBS (final concentration 1 µg/ml; 150 µl/well) for 30 min. Cells were washed three times with PBS and resuspended in 120 µl of FACS Flow (BD Bioscience). BODIPY 493/504 fluorescence was analyzed using a BD FACSCalibur flow cytometer with a 96-well plate high throughput autosampler. 50,000 events were analyzed per strain. In total 5127 strains were analyzed.

### Statistical and enrichment analysis

Data from the genome-wide screen were corrected for plate-to-plate variation and fat content in stationary phase (T0) by fitting a linear regression model with the measured BODIPY493/503-fluorescence intensity after 5 h growth (T5) as the response, the positive control values (WT; T0, T5), the negative control values (*tgl3*Δ; T0, T5), and the baseline BODIPY493/503-

fluorescence intensity values (T0) as covariates. Plots of residuals from this regression model versus the processing order, the date of processing and the plate number showed no systematic deviations, indicating no influence of these factors. The residuals from this linear regression were used as corrected intensity values and ranked. As compared to the initial ranking of raw values only some minor changes in ranking were observed. A non-parametric bootstrap experiment with 1000 replications was performed to assess the random variability of ranks. Overall, rankings showed small variability, with non-parametric 95% confidence intervals having lengths of <10 ranks for most of the top 50 yeast strains. Enrichment analysis of the ranked dataset was conducted based on gene ontology terms using the Gene Ontology enRIchment anaLysis and vizuaLizAtion (GOrilla) tool (Eden et al., 2009).

To display continuous data in groups, means were used. Statistical significance of difference between groups was determined using the two-tailed Student's *t*-test.

### Fluorescence microscopy

Cells were grown in SC medium containing 2% glucose to stationary phase. Where indicated, cells were diluted into fresh medium in the presence of 10 µg/ml cerulenin. The cells were collected at the indicated time points by centrifugation (5 min 4000 ***g*** 4°C) and washed once with PBS buffer. For staining of LDs, aliquots of cells were incubated with BODIPY493/503 (final concentration 1 µg/ml) for 15 min at 30°C, followed by washing twice with PBS before imaging. Images were acquired using an imaging system (Deltavision Elite; GE Healthcare) based on an inverted microscope (model IX-71; Olympus) equipped with an UAPON 100× (1.49 NA) oil immersion objective, an InsightSSI light source (Applied precision), excitation and emission filters for FITC, and a CoolSNAP $HQ^2$ CCD camera (Photometrics). Stacks with 0.35 µm spacing were imaged. For visualization of lipophagy during growth resumption (Fig. 5C), cells were grown to stationary phase in SC medium containing 2% glucose. Cells were diluted into fresh medium in the presence of cerulenin and FM4-64 (30 µM) for 1 h, washed with the corresponding medium and further incubated for 1 h in medium containing cerulenin without FM4-64. BODIPY493/503 was added for the last 30 min. After washing three times with PBS, cells were analyzed by fluorescence microscopy. Alternatively, LD autophagy during growth resumption was assessed in cells expressing the LD marker protein Erg6-GFP, co-labeled with FM4-64 (Fig. S3A). For fluorescence microscopy analysis in Fig. 6G, yeast cells expressing red fluorescent protein (RFP)-tagged Erg6p and GFP-tagged C1δ–domain from plasmids were grown in SC medium, 2% glucose, lacking leucine and uracil to stationary phase. Where indicated, cells were diluted into fresh medium in the presence of 10 µg/ml cerulenin. The cells were harvested by centrifugation and washed once before imaging. Images were acquired using a Zeiss LSM 880 inverted microscope equipped with a 63× (1.4 NA) oil objective and Zen.2 software. Where indicated, stacks with 0.4 µm spacing were imaged. Images were processed using ImageJ (National Institutes of Health) and Adobe Photoshop CC. Maximum projections are shown in Figs 2, 4 and 6.

### Lipidome analysis by mass spectrometry

Lipidome analysis was done as described previously (Almeida et al., 2015; Ejsing et al., 2009). In brief, cells were grown in SC medium containing 2% glucose for 24 h to reach stationary phase. Cells (10 OD units) were harvested at stationary phase and at the indicated time points after diluting stationary phase cells into fresh medium containing 10 µg/ml cerulenin. Cells were washed once and lipid analysis was performed using a Triversa NanoMate ion source (Advion Bioscience, Inc.) coupled to an Orbitrap Fusion Tribrid mass spectrometer (Thermo Fisher Scientific), as previously described (Almeida et al., 2015). For targeted lipid analysis of DAGs (Fig. 6B), 10 OD units of cells were washed once in ice-cold water and lipids were extracted as previously described (Markgraf et al., 2014), after addition of internal standard (d5 17:0 DAG, Avanti Polar lipids). Lipid extracts were dried under a stream of nitrogen and resuspended in methanol. Lipid analytes were separated using a Phenomenex Luna Omega column (1.6 µm 100A; Phenomenex, CA) on an Infinity 1290 HPLC system (Agilent Technologies, CA) and were analyzed by multiple reaction monitoring on a triplequadrupole mass spectrometer (Agilent 6495; Agilent Technologies), operated in positive ion mode.

### Total protein extraction from yeast

To quantify protein content of yeast cells, protein extracts of the indicated strains were generated by alkaline lysis. The OD of precultures was measured and cells (2 OD units) were lysed at in 0.25 M NaOH, 140 mM β-mercaptoethanol, 3 mM phenylmethylsulfonyl fluoride (PMSF). After 10 min incubation on ice, samples were subjected to trichloroacetic acid precipitation followed by acetone wash. SDS sample buffer was added and equal amounts of protein were analyzed by SDS-PAGE and western blotting. Anti-HA (mouse monoclonal clone 16B12, 1:1000, MMS-101R, BioLegend) and Anti-Pgk1 (mouse monoclonal clone 22C5D8, 1:5000, 459250, Thermo Fisher Scientific) antibodies were used.

#### Acknowledgements

We thank Markus Babst and Vanina Zaremberg for plasmids, Christian Ungermann and Kathrin Auffahrt for support using the Deltavision microscope, Manuel Hertel for technical support, the cellular morphology unit (DDZ) for help using the ZSM880 imaging system and Robin Klemm and Juliane Ahlers for critically reading the manuscript.

#### Competing interests

The authors declare no competing or financial interests.

#### Author contributions

Conceptualization: M.R., D.F.M.; Methodology: S.O., M.D.F., F.M., C.S.E., O.K., D.F.M.; Formal analysis: F.M., C.S.E., O.K., D.F.M.; Investigation: S.O., M.D.F., F.M., C.S.E., D.F.M.; Resources: M.R.; Data curation: C.S.E., O.K., D.F.M.; Writing - original draft: D.F.M.; Writing - review & editing: S.O., M.D.F., F.M., C.S.E., O.K., M.R., D.F.M.; Supervision: C.S.E., M.R., D.F.M.; Project administration: D.F.M.; Funding acquisition: M.R.

#### Funding

This work was supported by the Ministerium für Innovation, Wissenschaft und Forschung des Landes Nordrhein-Westfalen (MIWF NRW) and the Bundesministerium für Gesundheit (BMG). This study was supported in part by a grant of the Bundesministerium für Bildung und Forschung (BMBF) to the German Center for Diabetes Research (DZD e.V.). C.S.E. is supported by the VILLUM Fonden [grant number VKR023439 to C.S.E.] and the VILLUM Center for Bioanalytical Sciences [grant number VKR023179 to C.S.E.]. D.F.M. is supported in part by funding from the Deutsche Forschungsgemeinschaft (DFG; MA 7557/2-1).

#### Supplementary information

Supplementary information available online at
http://jcs.biologists.org/lookup/doi/10.1242/jcs.213876.supplemental

#### References

**Adeyo, O., Horn, P. J., Lee, S. K., Binns, D. D., Chandrahas, A., Chapman, K. D. and Goodman, J. M.** (2011). The yeast lipin orthologue Pah1p is important for biogenesis of lipid droplets. *J. Cell Biol.* **192**, 1043-1055.

**Almeida, R., Pauling, J. K., Sokol, E., Hannibal-Bach, H. K. and Ejsing, C. S.** (2015). Comprehensive lipidome analysis by shotgun lipidomics on a hybrid quadrupole-orbitrap-linear ion trap mass spectrometer. *J. Am. Soc. Mass Spectrom.* **26**, 133-148.

**Barbosa, A. D. and Siniossoglou, S.** (2017). Function of lipid droplet-organelle interactions in lipid homeostasis. *Biochim. Biophys. Acta* **1864**, 1459-1468.

**Barbosa, A. D., Sembongi, H., Su, W.-M., Abreu, S., Reggiori, F., Carman, G. M. and Siniossoglou, S.** (2015). Lipid partitioning at the nuclear envelope controls membrane biogenesis. *Mol. Biol. Cell* **26**, 3641-3657.

**Bouchez, I., Pouteaux, M., Canonge, M., Genet, M., Chardot, T., Guillot, A. and Froissard, M.** (2015). Regulation of lipid droplet dynamics in Saccharomyces cerevisiae depends on the Rab7-like Ypt7p, HOPS complex and V1-ATPase. *Biol. Open* **4**, 764-775.

**Bowers, K. and Stevens, T. H.** (2005). Protein transport from the late Golgi to the vacuole in the yeast Saccharomyces cerevisiae. *Biochim. Biophys. Acta* **1744**, 438-454.

**Buhman, K. K., Chen, H. C. and Farese, R. V., Jr.** (2001). The enzymes of neutral lipid synthesis. *J. Biol. Chem.* **276**, 40369-40372.

**Castellano, B. M., Thelen, A. M., Moldavski, O., Feltes, M. K., van der Welle, R. E. N., Mydock-McGrane, L., Jiang, X., van Eijkeren, R. J., Davis, O. B., Louie, S. M. et al.** (2017). Lysosomal cholesterol activates mTORC1 via an SLC38A9-Niemann-Pick C1 signaling complex. *Science* **355**, 1306-1311.

**Coonrod, E. M. and Stevens, T. H.** (2010). The yeast vps class E mutants: the beginning of the molecular genetic analysis of multivesicular body biogenesis. *Mol. Biol. Cell* **21**, 4057-4060.

**Czabany, T., Athenstaedt, K. and Daum, G.** (2007). Synthesis, storage and degradation of neutral lipids in yeast. *Biochim. Biophys. Acta* **1771**, 299-309.

**De Virgilio, C. and Loewith, R.** (2006). The TOR signalling network from yeast to man. *Int. J. Biochem. Cell Biol.* **38**, 1476-1481.
**Di Como, C. J. and Arndt, K. T.** (1996). Nutrients, via the Tor proteins, stimulate the association of Tap42 with type 2A phosphatases. *Genes Dev.* **10**, 1904-1916.
**Dimaano, C., Jones, C. B., Hanono, A., Curtiss, M. and Babst, M.** (2008). Ist1 regulates Vps4 localization and assembly. *Mol. Biol. Cell* **19**, 465-474.
**Drose, S. and Altendorf, K.** (1997). Bafilomycins and concanamycins as inhibitors of V-ATPases and P-ATPases. *J. Exp. Biol.* **200**, 1-8.
**Dubots, E., Cottier, S., Péli-Gulli, M.-P., Jaquenoud, M., Bontron, S., Schneiter, R. and De Virgilio, C.** (2014). TORC1 regulates Pah1 phosphatidate phosphatase activity via the Nem1/Spo7 protein phosphatase complex. *PLoS ONE* **9**, e104194.
**Dubouloz, F., Deloche, O., Wanke, V., Cameroni, E. and De Virgilio, C.** (2005). The TOR and EGO protein complexes orchestrate microautophagy in yeast. *Mol. Cell* **19**, 15-26.
**Eaton, J. M., Mullins, G. R., Brindley, D. N. and Harris, T. E.** (2013). Phosphorylation of lipin 1 and charge on the phosphatidic acid head group control its phosphatidic acid phosphatase activity and membrane association. *J. Biol. Chem.* **288**, 9933-9945.
**Eden, E., Navon, R., Steinfeld, I., Lipson, D. and Yakhini, Z.** (2009). GOrilla: a tool for discovery and visualization of enriched GO terms in ranked gene lists. *BMC Bioinformatics* **10**, 48.
**Ejsing, C. S., Sampaio, J. L., Surendranath, V., Duchoslav, E., Ekroos, K., Klemm, R. W., Simons, K. and Shevchenko, A.** (2009). Global analysis of the yeast lipidome by quantitative shotgun mass spectrometry. *Proc. Natl. Acad. Sci. USA* **106**, 2136-2141.
**Fakas, S., Konstantinou, C. and Carman, G. M.** (2011). DGK1-encoded diacylglycerol kinase activity is required for phospholipid synthesis during growth resumption from stationary phase in Saccharomyces cerevisiae. *J. Biol. Chem.* **286**, 1464-1474.
**Fei, W. and Yang, H.** (2012). Genome-wide screens for gene products regulating lipid droplet dynamics. *Methods Cell Biol.* **108**, 303-316.
**Forgac, M.** (2007). Vacuolar ATPases: rotary proton pumps in physiology and pathophysiology. *Nat. Rev. Mol. Cell Biol.* **8**, 917-929.
**Fujimoto, T. and Parton, R. G.** (2011). Not just fat: the structure and function of the lipid droplet. *Cold Spring Harb. Perspect. Biol.* **3**, a004838.
**Ganesan, S., Shabits, B. N. and Zaremberg, V.** (2015). Tracking Diacylglycerol and Phosphatidic acid pools in budding yeast. *Lipid Insights* **8**, 75-85.
**Gluchowski, N. L., Becuwe, M., Walther, T. C. and Farese, R. V. Jr.** (2017). Lipid droplets and liver disease: from basic biology to clinical implications. *Nat. Rev. Gastroenterol. Hepatol.* **14**, 343-355.
**Guo, Y., Walther, T. C., Rao, M., Stuurman, N., Goshima, G., Terayama, K., Wong, J. S., Vale, R. D., Walter, P. and Farese, R. V.** (2008). Functional genomic screen reveals genes involved in lipid-droplet formation and utilization. *Nature* **453**, 657-661.
**Han, G.-S., O'Hara, L., Siniossoglou, S. and Carman, G. M.** (2008). Characterization of the yeast DGK1-encoded CTP-dependent diacylglycerol kinase. *J. Biol. Chem.* **283**, 20443-20453.
**Heitman, J., Movva, N. R. and Hall, M. N.** (1991). Targets for cell cycle arrest by the immunosuppressant rapamycin in yeast. *Science* **253**, 905-909.
**Helle, S. C. J., Kanfer, G., Kolar, K., Lang, A., Michel, A. H. and Kornmann, B.** (2013). Organization and function of membrane contact sites. *Biochim. Biophys. Acta* **1833**, 2526-2541.
**Henne, W. M., Buchkovich, N. J. and Emr, S. D.** (2011). The ESCRT pathway. *Dev. Cell* **21**, 77-91.
**Henne, W. M., Zhu, L., Balogi, Z., Stefan, C., Pleiss, J. A. and Emr, S. D.** (2015). Mdm1/Snx13 is a novel ER-endolysosomal interorganelle tethering protein. *J. Cell Biol.* **210**, 541-551.
**Inokoshi, J., Tomoda, H., Hashimoto, H., Watanabe, A., Takeshima, H. and Ōmura, S.** (1994). Cerulenin-resistant mutants of Saccharomyces cerevisiae with an altered fatty acid synthase gene. *Mol. Gen. Genet.* **244**, 90-96.
**Jacinto, E., Loewith, R., Schmidt, A., Lin, S., Rüegg, M. A., Hall, A. and Hall, M. N.** (2004). Mammalian TOR complex 2 controls the actin cytoskeleton and is rapamycin insensitive. *Nat. Cell Biol.* **6**, 1122-1128.
**Jain, A. and Holthuis, J. C. M.** (2017). Membrane contact sites, ancient and central hubs of cellular lipid logistics. *Biochim. Biophys. Acta* **1864**, 1450-1458.
**Jin, Y. and Weisman, L. S.** (2015). The vacuole/lysosome is required for cell-cycle progression. *eLife* **4**, e08160.
**Kane, P. M.** (2006). The where, when, and how of organelle acidification by the yeast vacuolar H+-ATPase. *Microbiol. Mol. Biol. Rev.* **70**, 177-191.
**Kohlwein, S. D., Veenhuis, M. and van der Klei, I. J.** (2013). Lipid droplets and peroxisomes: key players in cellular lipid homeostasis or a matter of fat–store 'em up or burn 'em down. *Genetics* **193**, 1-50.
**Kurat, C. F., Natter, K., Petschnigg, J., Wolinski, H., Scheuringer, K., Scholz, H., Zimmermann, R., Leber, R., Zechner, R. and Kohlwein, S. D.** (2006). Obese yeast: triglyceride lipolysis is functionally conserved from mammals to yeast. *J. Biol. Chem.* **281**, 491-500.
**Lamming, D. W. and Sabatini, D. M.** (2013). A Central role for mTOR in lipid homeostasis. *Cell Metab.* **18**, 465-469.
**Lankester, D. L., Brown, A. M. and Zammit, V. A.** (1998). Use of cytosolic triacylglycerol hydrolysis products and of exogenous fatty acid for the synthesis of triacylglycerol secreted by cultured rat hepatocytes. *J. Lipid Res.* **39**, 1889-1895.
**Leber, R., Zinser, E., Zellnig, G., Paltauf, F. and Daum, G.** (1994). Characterization of lipid particles of the yeast, Saccharomyces cerevisiae. *Yeast* **10**, 1421-1428.
**Loewith, R., Jacinto, E., Wullschleger, S., Lorberg, A., Crespo, J. L., Bonenfant, D., Oppliger, W., Jenoe, P. and Hall, M. N.** (2002). Two TOR complexes, only one of which is rapamycin sensitive, have distinct roles in cell growth control. *Mol. Cell* **10**, 457-468.
**Longtine, M. S., McKenzie, A., III, Demarini, D. J., Shah, N. G., Wach, A., Brachat, A., Philippsen, P. and Pringle, J. R.** (1998). Additional modules for versatile and economical PCR-based gene deletion and modification in Saccharomyces cerevisiae. *Yeast* **14**, 953-961.
**Madeira, J. B., Masuda, C. A., Maya-Monteiro, C. M., Matos, G. S., Montero-Lomelí, M. and Bozaquel-Morais, B. L.** (2015). TORC1 inhibition induces lipid droplet replenishment in yeast. *Mol. Cell. Biol.* **35**, 737-746.
**Malia, P. C. and Ungermann, C.** (2016). Vacuole membrane contact sites and domains: emerging hubs to coordinate organelle function with cellular metabolism. *Biochem. Soc. Trans.* **44**, 528-533.
**Markgraf, D. F., Klemm, R. W., Junker, M., Hannibal-Bach, H. K., Ejsing, C. S. and Rapoport, T. A.** (2014). An ER protein functionally couples neutral lipid metabolism on lipid droplets to membrane lipid synthesis in the ER. *Cell Rep.* **6**, 44-55.
**Markgraf, D. F., Al-Hasani, H. and Lehr, S.** (2016). Lipidomics-reshaping the analysis and perception of type 2 diabetes. *Int. J. Mol. Sci.* **17**, 1841.
**Martínez-Muñoz, G. A. and Kane, P.** (2008). Vacuolar and plasma membrane proton pumps collaborate to achieve cytosolic pH homeostasis in yeast. *J. Biol. Chem.* **283**, 20309-20319.
**Menon, D., Salloum, D., Bernfeld, E., Gorodetsky, E., Akselrod, A., Frias, M. A., Sudderth, J., Chen, P.-H., DeBerardinis, R. and Foster, D. A.** (2017). Lipid sensing by mTOR complexes via de novo synthesis of phosphatidic acid. *J. Biol. Chem.* **292**, 6303-6311.
**Michaillat, L. and Mayer, A.** (2013). Identification of genes affecting vacuole membrane fragmentation in Saccharomyces cerevisiae. *PLoS ONE* **8**, e54160.
**Michaillat, L., Baars, T. L. and Mayer, A.** (2012). Cell-free reconstitution of vacuole membrane fragmentation reveals regulation of vacuole size and number by TORC1. *Mol. Biol. Cell* **23**, 881-895.
**Mima, J., Hickey, C. M., Xu, H., Jun, Y. and Wickner, W.** (2008). Reconstituted membrane fusion requires regulatory lipids, SNAREs and synergistic SNARE chaperones. *EMBO J.* **27**, 2031-2042.
**Miner, G. E., Starr, M. L., Hurst, L. R. and Fratti, R. A.** (2017). Deleting the DAG kinase Dgk1 augments yeast vacuole fusion through increased Ypt7 activity and altered membrane fluidity. *Traffic* **18**, 315-329.
**Müller, M., Schmidt, O., Angelova, M., Faserl, K., Weys, S., Kremser, L., Pfaffenwimmer, T., Dalik, T., Kraft, C., Trajanoski, Z. et al.** (2015). The coordinated action of the MVB pathway and autophagy ensures cell survival during starvation. *eLife* **4**, e07736.
**Natter, K., Leitner, P., Faschinger, A., Wolinski, H., McCraith, S., Fields, S. and Kohlwein, S. D.** (2005). The spatial organization of lipid synthesis in the yeast Saccharomyces cerevisiae derived from large scale green fluorescent protein tagging and high resolution microscopy. *Mol. Cell. Proteomics* **4**, 662-672.
**Nguyen, T. T., Lewandowska, A., Choi, J.-Y., Markgraf, D. F., Junker, M., Bilgin, M., Ejsing, C. S., Voelker, D. R., Rapoport, T. A. and Shaw, J. M.** (2012). Gem1 and ERMES do not directly affect phosphatidylserine transport from ER to mitochondria or mitochondrial inheritance. *Traffic* **13**, 880-890.
**Oelkers, P., Cromley, D., Padamsee, M., Billheimer, J. T. and Sturley, S. L.** (2002). The DGA1 gene determines a second triglyceride synthetic pathway in yeast. *J. Biol. Chem.* **277**, 8877-8881.
**Oku, M., Maeda, Y., Kagohashi, Y., Kondo, T., Yamada, M., Fujimoto, T. and Sakai, Y.** (2017). Evidence for ESCRT- and clathrin-dependent microautophagy. *J. Cell Biol.* **216**, 3263-3274.
**Orij, R., Urbanus, M. L., Vizeacoumar, F. J., Giaever, G., Boone, C., Nislow, C., Brul, S. and Smits, G. J.** (2012). Genome-wide analysis of intracellular pH reveals quantitative control of cell division rate by pH(c) in Saccharomyces cerevisiae. *Genome Biol.* **13**, R80.
**Pan, X., Roberts, P., Chen, Y., Kvam, E., Shulga, N., Huang, K., Lemmon, S. and Goldfarb, D. S.** (2000). Nucleus-vacuole junctions in Saccharomyces cerevisiae are formed through the direct interaction of Vac8p with Nvj1p. *Mol. Biol. Cell* **11**, 2445-2457.
**Penno, A., Hackenbroich, G. and Thiele, C.** (2013). Phospholipids and lipid droplets. *Biochim. Biophys. Acta* **1831**, 589-594.
**Peterson, T. R., Sengupta, S. S., Harris, T. E., Carmack, A. E., Kang, S. A., Balderas, E., Guertin, D. A., Madden, K. L., Carpenter, A. E., Finck, B. N. et al.** (2011). mTOR complex 1 regulates lipin 1 localization to control the SREBP pathway. *Cell* **146**, 408-420.
**Porat, Z., Wender, N., Erez, O. and Kahana, C.** (2005). Mechanism of polyamine tolerance in yeast: novel regulators and insights. *Cell. Mol. Life Sci.* **62**, 3106-3116.

**Qiu, Y., Hassaninasab, A., Han, G.-S. and Carman, G. M.** (2016). Phosphorylation of Dgk1 Diacylglycerol kinase by Casein Kinase II regulates phosphatidic acid production in Saccharomyces cerevisiae. *J. Biol. Chem.* **291**, 26455-26467.
**Raymond, C. K., Howald-Stevenson, I., Vater, C. A. and Stevens, T. H.** (1992). Morphological classification of the yeast vacuolar protein sorting mutants: evidence for a prevacuolar compartment in class E vps mutants. *Mol. Biol. Cell* **3**, 1389-1402.
**Sasser, T., Qiu, Q.-S., Karunakaran, S., Padolina, M., Reyes, A., Flood, B., Smith, S., Gonzales, C. and Fratti, R. A.** (2012). Yeast lipin 1 orthologue pah1p regulates vacuole homeostasis and membrane fusion. *J. Biol. Chem.* **287**, 2221-2236.
**Singh, R., Kaushik, S., Wang, Y., Xiang, Y., Novak, I., Komatsu, M., Tanaka, K., Cuervo, A. M. and Czaja, M. J.** (2009). Autophagy regulates lipid metabolism. *Nature* **458**, 1131-1135.
**Sorensen, S. O., van den Hazel, H. B., Kielland-Brandt, M. C. and Winther, J. R.** (1994). pH-dependent processing of yeast procarboxypeptidase Y by proteinase A in vivo and in vitro. *Eur. J. Biochem.* **220**, 19-27.
**Starr, M. L., Hurst, L. R. and Fratti, R. A.** (2016). Phosphatidic acid sequesters Sec18p from cis-SNARE complexes to inhibit priming. *Traffic* **17**, 1091-1109.
**Stauffer, B. and Powers, T.** (2015). Target of rapamycin signaling mediates vacuolar fission caused by endoplasmic reticulum stress in Saccharomyces cerevisiae. *Mol. Biol. Cell* **26**, 4618-4630.
**Szymanski, K. M., Binns, D., Bartz, R., Grishin, N. V., Li, W.-P., Agarwal, A. K., Garg, A., Anderson, R. G. W. and Goodman, J. M.** (2007). The lipodystrophy protein seipin is found at endoplasmic reticulum lipid droplet junctions and is important for droplet morphology. *Proc. Natl. Acad. Sci. USA* **104**, 20890-20895.
**Takeda, E., Jin, N., Itakura, E., Kira, S., Kamada, Y., Weisman, L. S., Noda, T. and Matsuura, A.** (2018). Vacuole-mediated selective regulation of TORC1-Sch9 signaling following oxidative stress. *Mol. Biol. Cell* **29**, 510-522.
**Tilg, H., Moschen, A. R. and Roden, M.** (2017). NAFLD and diabetes mellitus. *Nat. Rev. Gastroenterol. Hepatol.* **14**, 32-42.
**Toschi, A., Lee, E., Xu, L., Garcia, A., Gadir, N. and Foster, D. A.** (2009). Regulation of mTORC1 and mTORC2 complex assembly by phosphatidic acid: competition with rapamycin. *Mol. Cell. Biol.* **29**, 1411-1420.
**Urban, J., Soulard, A., Huber, A., Lippman, S., Mukhopadhyay, D., Deloche, O., Wanke, V., Anrather, D., Ammerer, G., Riezman, H. et al.** (2007). Sch9 is a major target of TORC1 in Saccharomyces cerevisiae. *Mol. Cell* **26**, 663-674.
**van Zutphen, T., Todde, V., de Boer, R., Kreim, M., Hofbauer, H. F., Wolinski, H., Veenhuis, M., van der Klei, I. J. and Kohlwein, S. D.** (2014). Lipid droplet autophagy in the yeast Saccharomyces cerevisiae. *Mol. Biol. Cell* **25**, 290-301.
**Walther, T. C. and Farese, R. V. Jr.** (2012). Lipid droplets and cellular lipid metabolism. *Annu. Rev. Biochem.* **81**, 687-714.
**Wang, C.-W.** (2014). Stationary phase lipophagy as a cellular mechanism to recycle sterols during quiescence. *Autophagy* **10**, 2075-2076.
**Wang, C.-W., Miao, Y.-H. and Chang, Y.-S.** (2014). A sterol-enriched vacuolar microdomain mediates stationary phase lipophagy in budding yeast. *J. Cell Biol.* **206**, 357-366.
**Wickner, W.** (2010). Membrane fusion: five lipids, four SNAREs, three chaperones, two nucleotides, and a Rab, all dancing in a ring on yeast vacuoles. *Annu. Rev. Cell Dev. Biol.* **26**, 115-136.
**Wiggins, D. and Gibbons, G. F.** (1992). The lipolysis/esterification cycle of hepatic triacylglycerol. Its role in the secretion of very-low-density lipoprotein and its response to hormones and sulphonylureas. *Biochem. J.* **284**, 457-462.
**Yamashiro, C. T., Kane, P. M., Wolczyk, D. F., Preston, R. A. and Stevens, T. H.** (1990). Role of vacuolar acidification in protein sorting and zymogen activation: a genetic analysis of the yeast vacuolar proton-translocating ATPase. *Mol. Cell. Biol.* **10**, 3737-3749.
**Yoon, M.-S., Sun, Y., Arauz, E., Jiang, Y. and Chen, J.** (2011). Phosphatidic acid activates mammalian target of rapamycin complex 1 (mTORC1) kinase by displacing FK506 binding protein 38 (FKBP38) and exerting an allosteric effect. *J. Biol. Chem.* **286**, 29568-29574.
**Young, B. P., Shin, J. J. H., Orij, R., Chao, J. T., Li, S. C., Guan, X. L., Khong, A., Jan, E., Wenk, M. R., Prinz, W. A. et al.** (2010). Phosphatidic acid is a pH biosensor that links membrane biogenesis to metabolism. *Science* **329**, 1085-1088.
**Zoncu, R., Bar-Peled, L., Efeyan, A., Wang, S., Sancak, Y. and Sabatini, D. M.** (2011). mTORC1 senses lysosomal amino acids through an inside-out mechanism that requires the vacuolar H(+)-ATPase. *Science* **334**, 678-683.